Delay-Throughput Performance of the Deep-Space Ka-band Link

Shervin Shambayati *

In this paper, performance of a first-in, first-out (FIFO), selective retransmission scheme for the deep-space Ka-band link is presented and compared to the performance of a comparable X-band link. In this analysis, 16 months of water vapor radiometer (WVR) and advanced water vapor radiometer (AWVR) data from the three Deep Space Network (DSN) Communication Complexes (DSCC) were used to emulate weather effects on X-band and Ka-band links from Mars. Mars Reconnaissance Orbiter (MRO) X-band and Ka-band telecommunications parameters were used for spacecraft telecommunications capabilities. One pass per week per complex was selected from MRO's Deep Space Network (DSN) schedule from April 1, 2006 to August 31, 2007 for a total of 207 passes (69 passes per complex) for this analysis. For each pass both X-band and Ka-band links were designed using at most two data rates so that the expected pass capacity would be maximized subject to a minimum availability requirement (MAR). In conjunction with the WVR/AWVR data, elevation profiles of the selected passes and models for the performance of the antennas in the DSN were used to emulate the performance of both links. It was assumed that the retransmission of the data takes place not on the same pass as the original transmission but during subsequent passes. The data collected before a pass was assumed to be a fraction of the expected capacity of the pass as calculated through the link design process. Infinite spacecraft storage was assumed to obtain an upper bound on the spacecraft storage requirement. The independent parameters of this analysis were MAR and the ratio of data collected before a pass to the expected pass capacity. Since the selected passes did not occur at regular intervals, the delay in this analysis was measured in terms of number of passes. The throughput was measured in terms of number of bits received successfully on the ground. The results indicate that reasonable delay performance could be achieved with very high throughput for relatively low MAR values for data collection to expected pass capacity ratio of around 97% for Ka-band. The results indicate that, except for very low average delay requirements, the Ka-band link provides more than twice the throughput of the X-band link for the same amount of power consumed by the spacecraft. In addition, the results indicate that the required storage onboard the spacecraft is not prohibitive and good performance could be achieved by using a buffer size less than three times the maximum amount of data collected before a pass.

Nomenclature

p_d Data Collection Factor

I. Introduction

Due to limited bandwidth alllocation in the 8.42 GHz X-band (only 50 MHz), future deep-space missions will use a 500 MHz allocation in the 32 GHz Ka-band for their downlink operations. Ka-band is much more

*Jet Propulsion Laboratory, California Institute of Technology

susceptible to adverse weather effects than X-band, so that for every dB of loss due to weather at X-band, a Ka-band link suffers approximately 4 dB of loss.[1] Therefore, a simple margin policy cannot assure data completeness without a significant reduction in data return, and the only practical way to guarantee data completeness is through retransmission of the lost data. Several issues must be considered when dealing with retransmissions. These include the bandwidth allocation for retransmissions, throughput of the system, the delay in the delivery of the data and the required storage on the spacecraft.

Originally, Mars Reconnaissance Orbiter (MRO) Ka-band Demonstration was to have provided data to evaluate these requirements. However, because of a failure in the Ka-band telemetry chain on the spacecraft,[1] the demonstration was indefinitely postponed. Therefore, the objectives of the demonstration had to be met through other means. Among the tools available for this purpose are water vapor radiometer (WVR) and advanced water vapor radiometer (AWVR) sky brightness temperature measurements at 31.4 GHz. These sky brightness temperature measurements can be converted to zenith atmospheric noise temperature (ZANT) measurements for both 32-GHz Ka-band and 8.42-GHz X-band.The ZANT measurements along with models for the gain and the equipment noise temperature for the Deep Space Network (DSN) antennas[2] then could be used to emulate the performance of either the Ka-band or the X-band link at any time for which the WVR/AWVR data are available. Such an emulation has been used to evaluate Ka-band continuity and completeness performance[3] using MRO Ka-band parameters and MRO's tracking schedule. In this paper, this emulation is used to evaluate the delay-throughput performance of both the X-band and the Ka-band links.

This paper is organized in the following manner. In Section II, assumptions and techniques used in this emulation are discussed. The results are presented in Section III. In Section IV, conclusions are reached and caveats are discussed.

II. Assumptions and Technical Background

Before the link delay-throughput performance could be characterized, assumptions made about the overall system characteristics have to be clarified. These include spacecraft telecommunications parameters, selection of the passes for emulation, link design approach, channel emulation, spacecraft data management and measures of performance.

II.A. Spacecraft Telecommunications Parameters

We have selected MRO's telecommunications parameters for our analysis. MRO Ka-band system has a 35-W RF power traveling-wave tube amplifier (TWTA) transmitting over a 3-m parabolic antenna producing an equivalent isotropic radiated power (EIRP) of 101.3 dBm. The input power consumption of the Ka-band TWTA is 80 W. The X-band system on MRO consists of a 100-W RF power TWTA transmitting over the same 3-m antenna producing an EIRP of 96.2 dBm. The input power to the X-band TWTA is 172 W. Both Ka-band and X-band use the same set of data rates as prescribed by *MRO Telecom Handbook*[a]. Note that the transmitted RF power at X-band is almost three times as great as the that for the Ka-band. The reason for this is the fact that, given the available data rates and the geometry considered for this study, the selected RF power levels provide roughly the same performance for both bands.

Due to the limitation on bandwidth and the decoding speed of the ground turbo decoder, a variety data rates and codes are used by the spacecraft. In our analysis, for a given data rate, we have selected the best possible code in terms of bit signal-to-noise ratio (E_b/N_0). Table 1 shows the information data rates and their associated channel codes as obtained through this process. All these codes are described in the CCSDS Channel Coding Green Book.[5]

Even though spacecraft antenna pointing losses could be significant at Ka-band, based on our experience with MRO Ka-band signal during MRO's cruise phase[4] these pointing losses for MRO are negligible, and

[a]Internal JPL Document. Not available to the public.

Table 1. MRO Data Rates and Associated Channel Codes

Information Data Rate (bps)	Channel Code
27846.76	Concatenated Coding
331397.95	(8920, 1/6) Turbo Code
497096.92	(8920, 1/6) Turbo Code
662795.89	(8920, 1/6) Turbo Code
745645.38	(8920, 1/2) Turbo Code
994193.84	(8920, 1/3) Turbo Code
1325591.78	(8920, 1/3) Turbo Code
1491290.75	(8920, 1/2) Turbo Code
1740422.20	Concatenated Coding
2610633.31	Concatenated Coding
2871696.64	Reed-Solomon-Only
3480844.41	Reed-Solomon-Only
5221266.61	Reed-Solomon-Only

therefore, are assumed to be zero.

II.B. Selection of Passes for Emulation

A period from April 1, 2006 through July 31, 2007 were selected for this analysis. Over this period, one pass per week per DSN complex was selected from the MRO DSN schedule. DSN Communication Complexes (DSCCs) are located at Goldstone, California; near Madrid, Spain and near Canberra, Australia. The passes were selected such that WVR/AWVR were available for their entire duration. Because of this, there were several weeks that no passes could be selected over a particular complex. In such cases, additional passes were selected in weeks before and/or after those weeks for that particular complex. Even though not all the passes selected were originally scheduled on Ka-band capable 34-m beam waveguide (BWG) antennas, for the purpose of this analysis, parameters for a Ka-band capable antenna at the selected complex were used. The Ka-band capable antennas at the DSN are Deep Space Station (DSS) 25 and DSS-26 at Goldstone, DSS-55 at Madrid and DSS-34 at Canberra.

II.C. Link Design

Both the Ka-band and the X-band links were designed using the approach outlined in[3] and.[6] Under this approach, for each pass, the link is designed with at most two data rates so that the expected data return is maximized subject to a minimum availability requirement (MAR). Monthly ZANT statistics at the three DSCCs for both X-band and Ka-band along with models for the DSN ground antenna performance parameters[2] were used to perform the necessary calculations. In this fashion, the data return on the link is maximized while the operational complexity is kept to a minimum (through the use of at most two data rates) and a minimum link reliability is maintained. Depending on the selected MAR, the data rates selected and the times at which the link uses those data rates could change. In Fig. 1, this is illustrated for the pass on day 2006-229 occuring over DSS-55. Furthermore, because the weather effects cause greater variations in the performance of Ka-band as a function of elevation and the EIRP, ground antenna gain and space losses are different for X-band and Ka-band, the Ka-band and X-band data rates for the same MAR value are usually not the same. This is illustrated in Fig. 2 for the pass over DSS-55 on day 2006-229. It should

be noted that for this analysis, occultation of the spacecraft behind Mars and scintillation effects caused by solar conjunction are ignored in order to simplify the analysis.

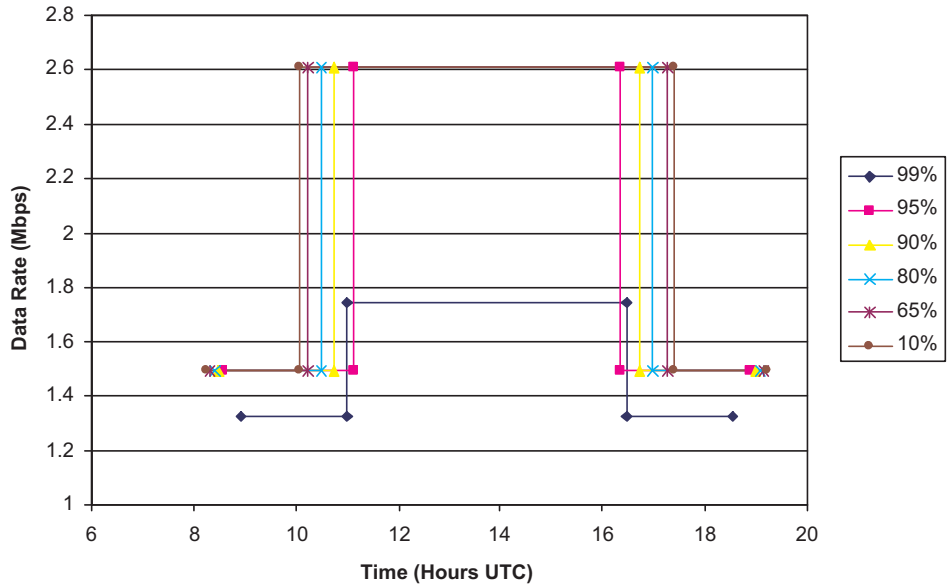

Figure 1. Designed Ka-band Link Data Rates for Different Minimum Availability Requirement (MAR) Values, Day 2006-229, DSS-55

II.D. Channel Emulation

Channel conditions were emulated using the WVR/AWVR data. In order to do so, 31.4-GHz zenith sky brightness temperatures obtained from the WVR/AWVR data were converted to ZANT values at 8.42 GHz and 32 GHz. For each pass, these values were used along with the models for 34-m BWG antenna performance at X-band and Ka-band[2] and the elevation profile for the pass to obtain the actual system gain-to-temperature ratio (G/T) at one minute intervals. It should be noted that the WVR/AWVR data are provided at intervals of roughly once every five minutes; therefore, a linear interpolation was used to obtain the ZANT data at one-minute intervals.

Once the actual G/T time series for a pass are obtained, they could be compared with the G/T required to close the link. Through this, the status of the link could be calculated at any time during the pass and the data return for the pass and the amount of data left in the spacecraft buffer could be determined. This is illustrated in Fig. 3.

Fig. 3 shows the performance of the Ka-band link emulated for day 2006-229 for DSS-55 for a link designed for 90% MAR. First, the required G/T is calculated based on the initial link design for 90% MAR (the green curve). Note that the required G/T is below 90% predicted G/T (the black curve) indicating that the design meets the minimum availability requirement of 90%. Next, the actual G/T is calculated from the WVR/AWVR data (the red curve). Finally, the status of the link is determined with the status being good when the actual G/T is greater than or equal to the required G/T and the status being bad when the actual G/T is less than the required G/T. The status of the link is indicated by the blue curve. From the status curve, based on the assumption about data management on the spacecraft (see II.E below), the amount of data received over the pass and the data left over in the buffer could be calculated. Note that this analysis

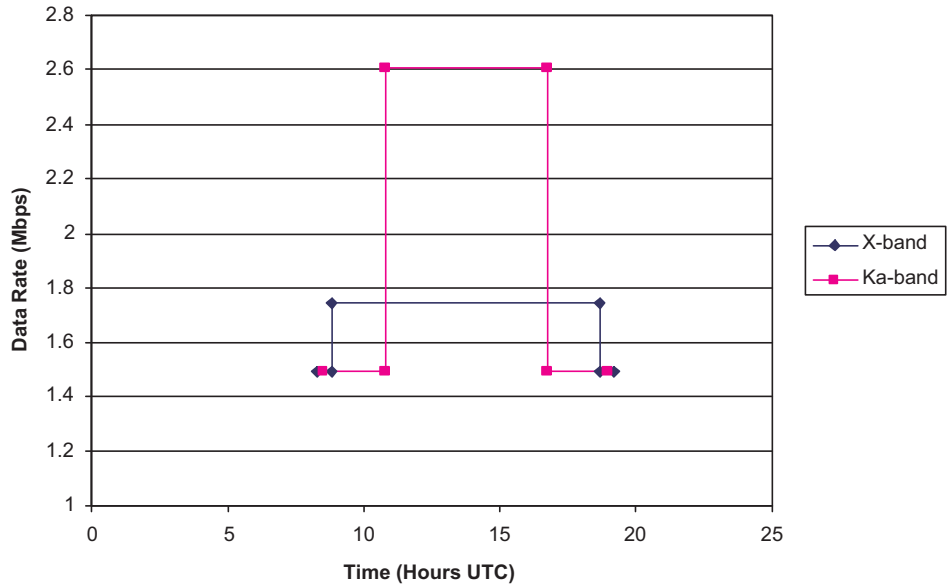

Figure 2. Designed X-band and Ka-band Data Rates, 90% MAR, Day 2006-229, DSS-55

ignores the normal errors that occur due to additive white gaussian noise in order to simplify the analysis. This methodology is valid because all the codes used have an essentially waterfall error rate curves where a few tenths of dBs could make the difference between total data loss and perfect data return.

II.E. Data Management

Two issues need to be addressed with regards to data management: how much data to collect and what data to transmit. In this analysis, we use the fact that the link design procedure provides the expected amount of data that could be successfully received during the pass. From queuing theory, it is well-known that in order to keep the amount of data in a queue (the buffer size) finite, it is necessary that the average data input rate for the buffer be less than the average processing rate of the server. Given this, we limit the amount of *new* data collected before a pass to a fraction (less than 1) of the *expected* data return for the pass. For example, if this fraction– the data collection factor p_d– is set to 0.95, before a pass with an expected data return of 1 Gbits, only 950 Mbits of new data is collected. By varying p_d, the loading of the link is changed and thus, delay and throughput of the link will vary. Note that this approach is not that different from current MRO X-band operational practices. MRO reserves 3% of its downlink capacity for retransmissions of the data that was not successfully received during previous passes, and new data collected is equal to 97% of the downlink capacity per pass.[b] For sake of simplicity, in our analysis, we assume that no data is collected during a pass as the spacecraft is transmitting.

For data transmission, we assume a slightly modified first-in-first-out (FIFO) policy. Under this approach, before the start of the pass, it is known what data will be transmitted during the pass (not in terms of content but rather in terms of its position in the buffer) with the older data transmitted before the newer data. If any of the transmitted data is lost during the pass, its retransmission has to occur during subsequent passes. It is assumed that the buffer is purged of all the data that were successfully received during the pass at the

[b]Conversation with Roy Gladden of MRO project.

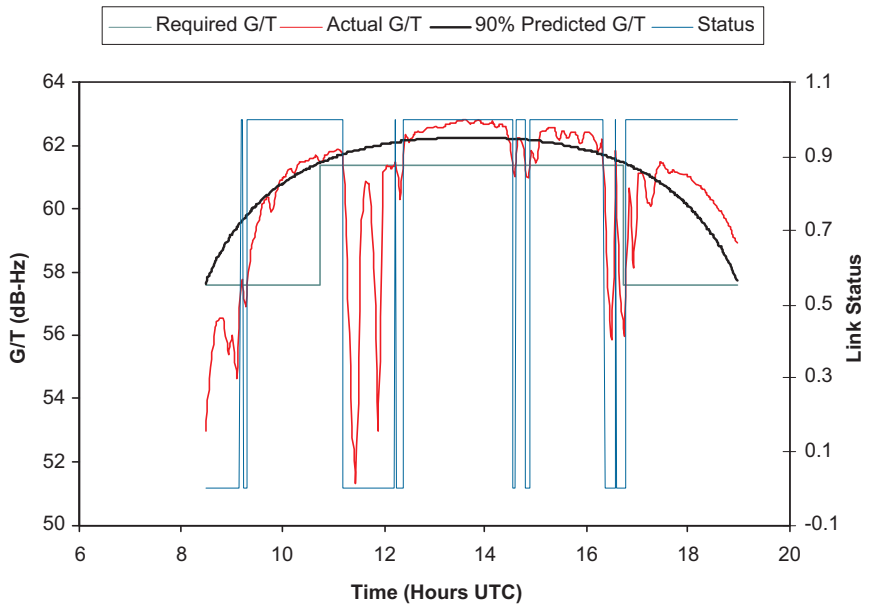

Figure 3. Predicted 90% G/T, Required G/T, Actual G/T and Link Status, Day 2006-229, DSS-55

end of the pass. This is illustrated in Fig. 4.

In Fig. 4, some of the data in the buffer is scheduled for transmission during the pass occuring from 12:00 to 20:00. From 12:25 to 14:00 the link suffers an outage which causes the data transmitted during that time not to be received correctly. Therefore, at the end of the pass, the spacecraft is commanded to purge its buffer of only the data that was received correctly (the green portion of the data). By the start of the next pass, the data that was not successfully received during the previous pass (the portion of data colored red) is scheduled for transmission first, followed by the data that was in the buffer during the previous pass but was not transmitted (the cyan data), followed by the new data that was collected after the previous pass (the magenta colored data). Note that the reception of the data that was not successfully received during the previous pass could be unsuccessful during the next pass. In our analysis, we assume an infinite buffer; therefore, the data is kept in the buffer until it is successfully received on the ground. Note that this approach is different from MRO's approach to data transmission. With MRO, for every pass, 97% of the downlink capacity is dedicated to the transmission of new data as opposed to our FIFO scheme.

II.F. Measures of Performance

As the title of this paper implies, the two main metrics of performance are delay and throughput. Because the passes are scheduled in an ad hoc manner, the delay is measured in terms of passes with a delay of one, indicating that a piece of data was transmitted on the pass before which it was collected. In our analysis we also obtain the delay distribution and average delay of the data in terms of passes. Throughput refers to the amount of data that received correctly on the ground.

The measure that is helpful in evaluating the storage requirements of the spacecraft is the maximum of the ratio of the buffer size at the beginning of the pass to the amount of data collected before the pass. This measure is useful because it is a normalized measure. The buffer size, as measured in number of bits, only relates to specific parameters that are used in this emulation. Through normalization, we can determine how

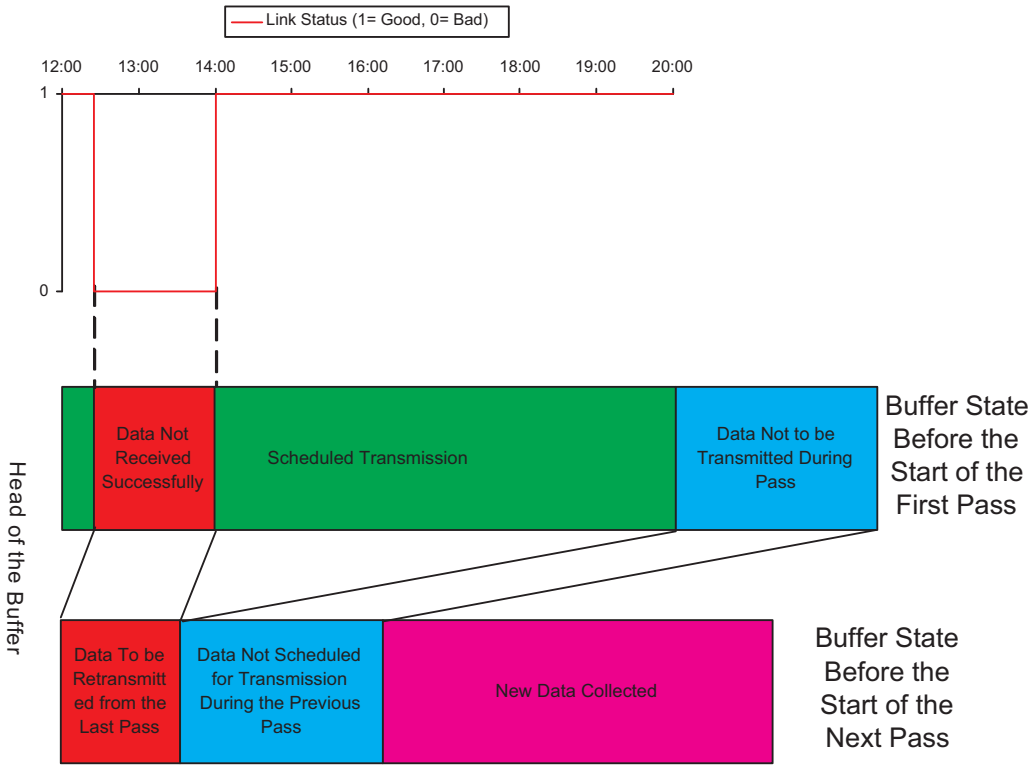

Figure 4. Illustration of the Buffer Management Mechanism

much storage relative to the amount of data that spacecraft collects is needed with Ka-band. This measure also, to some extent, counteracts the variability of the link. Because we are using actual MRO trajectory for our calculations, over time, the distance between Earth and the spacecraft and the duration and elevation of the passes at each complex vary. These cause variations in the capacity of the link; therefore, the amount data that is collected before each pass could vary significantly over time. These variations, in turn, could lead to misleading results with regards to the spacecraft storage requirements if no normalization is used. By using a normalized measure, the true effects of the weather on the spacecraft storage requirements could be assessed.

III. Results

III.A. Delay-Throughput

The two free parameters in this analysis were the MAR and the data collection factor. MAR values of 10%, 50%, 65%, 80%, 85%, 90%, 92.5%, 95%, 97.5% and 99% were selected for both X-band and Ka-band. For each MAR value, the delay-throughput performance was calculated for both X-band and Ka-band for data collection factors (p_d) of 0.5, 0.6, 0.7, 0.8, 0.85, 0.87, 0.9, 0.91, 0.92, 0.93, 0.94, 0.95, 0.96, 0.97, 0.98, 0.99, 0.994 and 1. There results of these calculations are shown in Figs. 5 and 6.

As seen from these figures, the higher throughputs are achieved by the lower MAR values while lower delays are achieved by the higher MAR values. This result is completely expected. A link with higher reliability is less susceptible to losses thus reducing the number of transmissions of the data for successful

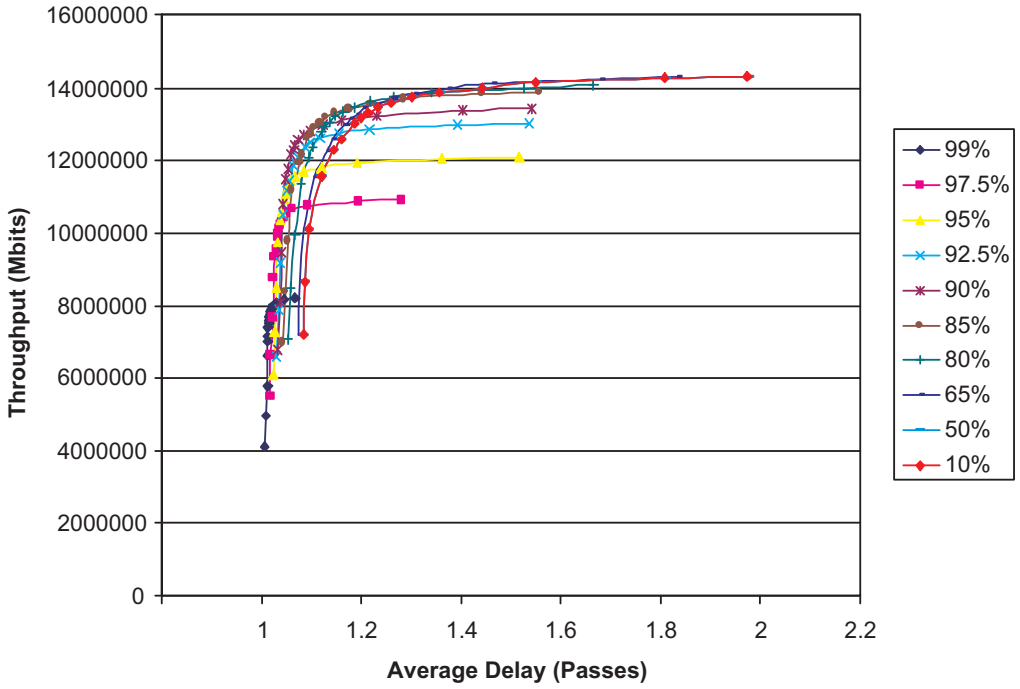

Figure 5. Ka-band Throughput vs. Average Delay in Passes for Different Minimum Availability Requirement Values

reception, and, by definition, links designed with the higher MAR values are more reliable. Conversely, higher throughputs are achieved by links with higher average capacity, and links with lower MAR values have a higher average capacity.[6]

Note that all delay-throughput curves display an asymptotic behavior in that for larger average delay values, a slight increase in the throughput is accompanied by a significant increase in the average delay. This is typical of heavily loaded queues. Since the capacity of the link is limited, there is a maximum throughput equal to its capacity that the link can support. However, as queuing theory tells us, to achieve a throughput equal to the link capacity for an infinite queue, the queue size has to approach infinity and thus the delay becomes infinite as well.

These figures also indicate that the delay-throughput performance of the Ka-band link varies significantly more than the delay-throughput performance of the X-band link as a function of MAR. This is due to the fact that the weather effects at Ka-band are more severe than those at the X-band, causing approximately 4 dB of loss at Ka-band for every dB of loss at X-band.[1] Therefore, the weather reliability at Ka-band costs significantly more than that at X-band in terms of channel capacity. A higher MAR value leads to a greater drop in the average channel capacity at Ka-band compared to X-band and a significant drop in channel capacity leads to a significant drop in the throughput performance of the link. Therefore, Ka-band curves display a greater variation in terms of throughput when the MAR is changed.

Another interesting observation is that, depending on the average delay, the MAR which provides the maximum throughput changes. When the average delay is low, the higher MAR curves provide better throughput. Conversely, when the average delay is high, the lower MAR curves provide better throughput. Because of this, the true delay-throughput performance of Ka-band and X-band links is defined by the upper envelope of the delay-throughput curves in Figs. 5 and 6, respectively. Fig. 7 shows these upper envelopes.

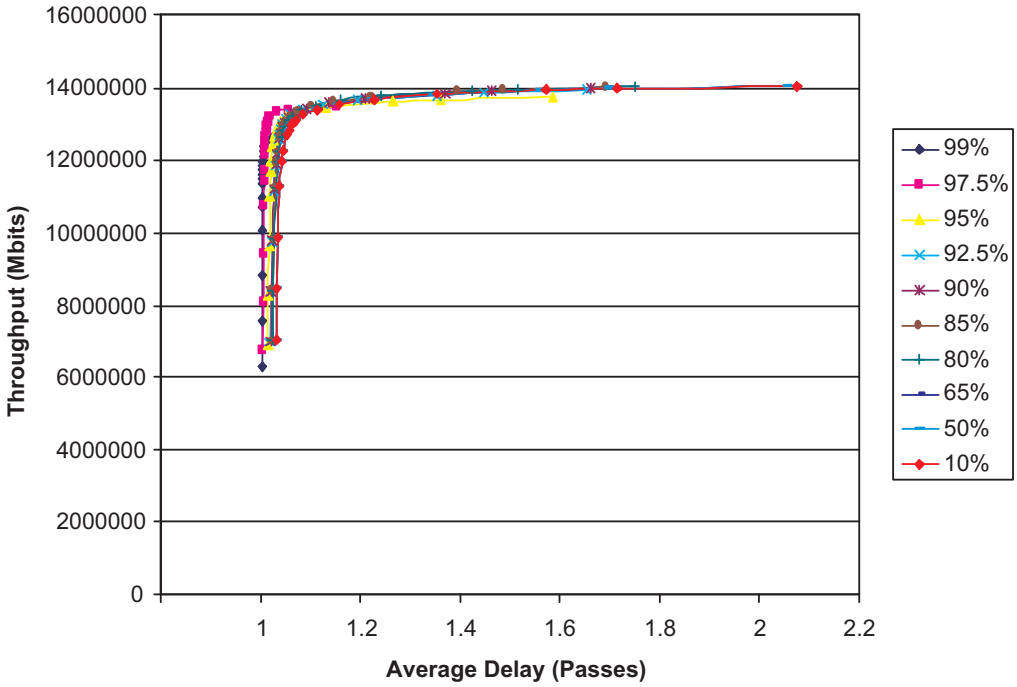

Figure 6. X-band Throughput vs. Average Delay in Passes for Different Minimum Availability Requirement Values

Fig. 7 indicates that while the maximum throughput offered by X-band and Ka-band are comparable, the X-band system can support higher throughputs for lower average delays. However, the reader is reminded that X-band requires 172 W of DC input power compared to only 80 W for Ka-band. Therefore, if the envelopes are normalized to the input power, Ka-band displays a significant advantage for all but the smallest average delay values (Fig. 8). For average delay values greater than 1.1, the Ka-band's throughput per watt is more than twice as large as the X-band's. It should be noted, however, that if having very small average delay is critical (for activities such as orbit insertion and entry-descent-landing operations) X-band still provides better performance than Ka-band.

III.B. Delay Distributions

In III.A the delay was discussed solely in terms of average delay. However, the shape of the delay distributions is important as well. If the delay distributions have a heavy tail, *i.e.*, they indicate that there is a possibility that some data may stay in the storage area for a long time (more than, say, ten passes) then, even though the average delay is acceptable, the overall delay performance maybe unacceptable. The results of our analysis, however, suggest that the delay distributions are well-behaved and that the average delay is a good measure of the overall distribution.

First, we consider the probability that a piece of data will stay in the spacecraft storage for a long time. Analyzing the delay distribution, the largest delay that was observed was seven passes; *i.e.*, in our emulation, regardless of MAR and p_d, no data took longer than seven passes to be received successfully. This delay only occurred for the Ka-band link with MARs of 10% and 50% for p_d values 1.0 and 0.994 and constituted the delay for less than 0.02% of the data.

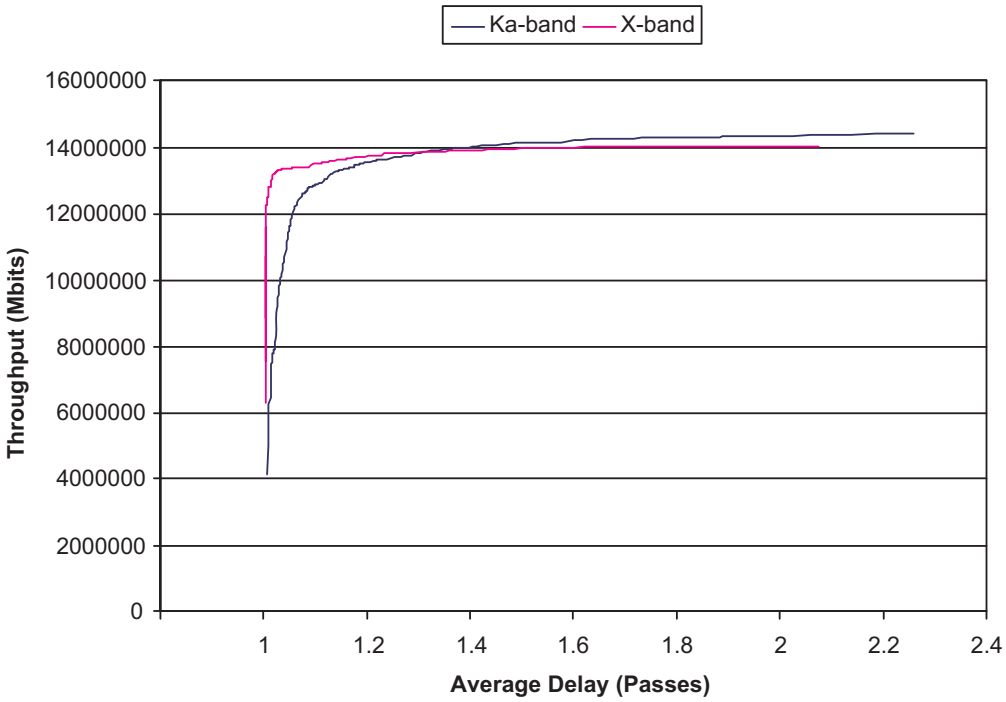

Figure 7. X-band and Ka-band Delay-Throughput Upper Envelopes

Next, we focus on the overall shape of the distribution and its overall sensitivity to changes in MAR and in p_d. Fig. 9 shows the variation in the delay distribution for the Ka-band link with a MAR 90% as p_d is varied. As expected, as the p_d increases, so does the probability that the delay is greater than one because the loading of the system has increased. Note that for this MAR value, even with a $p_d = 0.95$ more than 90% data is received on the first transmission. Fig. 10 shows the variation in the delay distribution for a Ka-band link with a $p_d = 0.97$ as the MAR is varied. In this case, even though the loading of the system is kept constant relative to the capacity of the link for all MAR values, lower MAR values exhibit higher delays. This is because with lower MAR values the link is more susceptible to link outages which cause more retransmissions.

Finally, we consider whether or not the average delay is a good measure of the overall shape of the delay distribution; *i.e.*, whether or not the delay distribution is characterized by a single parameter. Our initial analysis suggests that this is the case, although further analysis is recommended. We have looked at several delay distributions whose average delay values were roughly the same, and in all cases, both the shape of the distributions and the standard deviation of the distributions were also roughly the same. This is illustrated by the examples in Table 2 and Fig. 11. Note that there is very little frequency dependency and that for these examples the distributions are roughly the same regardless of the frequency band.

III.C. Buffer Size

As mentioned before, in our analysis we have assumed infinite storage in order to determine what is the necessary buffer size. However, because of variations in the Earth-to-Probe distance and the length of passes, the maximum buffer size observed is not a good measure of performance, and a better metric is the maximum of the ratio of the buffer size at beginning of the pass to the total amount of data collected before

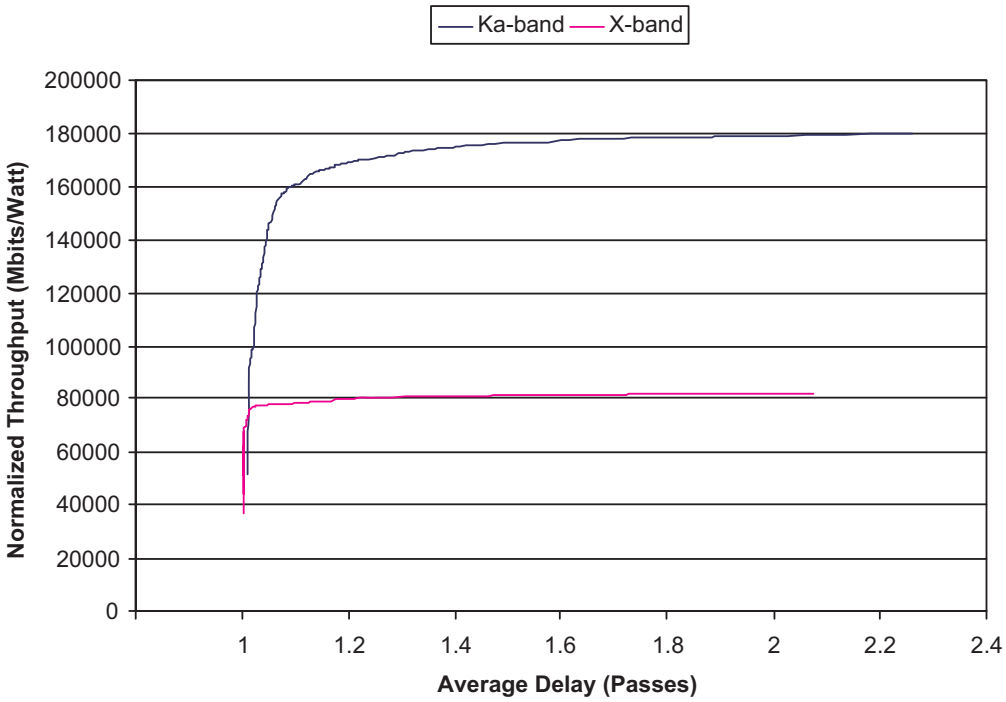

Figure 8. X-band and Ka-band Normalized Delay-Throughput Upper Envelopes

the pass. Figs. 12 and 13 show this metric for Ka-band and X-band, respectively, for different p_d and MAR values.

As seen from these figures, typically, the maximum ratio increases with a very high rate of increases when p_d is greater than 0.9. For p_d values less than 0.9 the trend is not so clear. This is because of the limited number of passes that are available. Since the metric is the maximum of a ratio that is calculated on a pass-by-pass basis, variations on the link performance and duration over a few passes could affect the metric greatly. This is illustrated in Fig. 14. In this figure, the buffer size at the start of the pass, the amount of data collected before the pass, the amount data received successfully during the pass and the ratio of the buffer size at the start of the pass to the amount of data collected before the pass for the Ka-band link designed for a MAR of 65% and a $p_d = 0.97$ are shown for seven consecutive passes. As seen from this figure, passes on days 2006-291, 2006-292 and 2006-297 suffer some losses. This is indicated by the fact that

Table 2. Delay Average and Standard Deviations for Different X-band and Ka-band Link Configurations with Similar Average Delays

Freq.	MAR	p_d	Avg. Delay	Delay Sd.
Ka	80%	0.96	1.216	1.297
Ka	10%	0.93	1.228	1.326
X	80%	0.98	1.239	1.327
X	10%	0.97	1.227	1.316

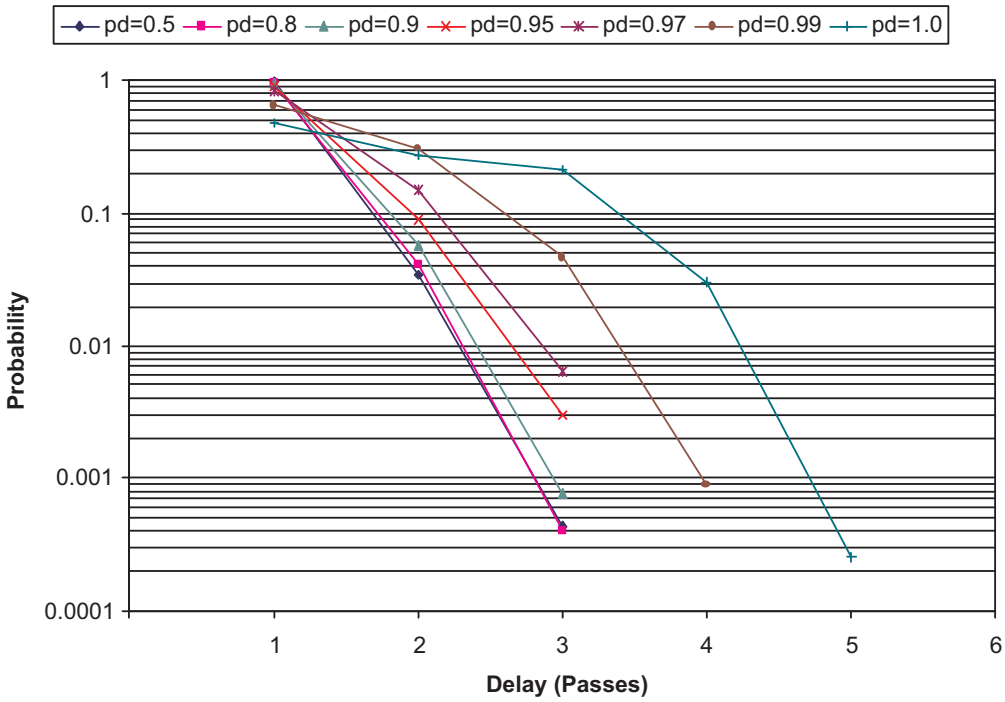

Figure 9. Ka-band Delay Distributions for MAR=90% and Different p_d Values

the amount of data received during the pass is less than the amount of data collected before the pass. This causes a build up of data in the buffer as seen from the curve indicating the buffer size before the pass. Passes on days 2006-301, 2006-302 and 2006-305 all successfully transmit more data than was collected before the start of the pass. However, because of the build up of the data during the previous three passes, the ratio of buffer size before the start of the pass to the amount of data collected before the pass is rather high. Note that, the maximum ratio is not achieve for the largest buffer size for the pass on day 2006-301 but rather it is achieved for the pass on 2006-302 where very little data was collected before the pass. The reason for this was that the pass on day 2006-302 was rather short due to the trajectory of the spacecraft relative to DSS-34 which caused a subsequent reduction in the capacity of the pass and the amount of data that was collected before the pass. This indicates that the maximum ratio is not a perfect metric and may overestimate the required buffer size. However, given the variation in the geometry of passes considered, this metric comes closest to capturing the storage requirements of the spacecraft.

It should be noted that for high MAR and p_d values, the maximum ratio of the buffer size at the start of the pass to the data collected before the pass is roughly the same for X-band and Ka-band. This is illustrated in Fig. 15. This figures show the maximum ratio as a function of MAR for p_d=0.97. As seen from this figure, for MAR values of 80% and above, X-band and Ka-band have roughly the same maximum ratio. Furthermore, this figure indicates that even for a p_d of 0.97, the storage requirement seems reasonable with the maximum ratio of less than 3 for both X-band and Ka-band. This means that a spacecraft storage whose capacity is greater than three times the maximum amount of data it collects between passes probably will not see a buffer overflow. The reader should be reminded, however, that current X-band missions do not have very much storage because they operate under regimes that the data delivery is almost 100% guaranteed, *i.e.*, the effective MAR for the link is nearly 100%. As Fig. 15 indicates, under such circumstances, storage

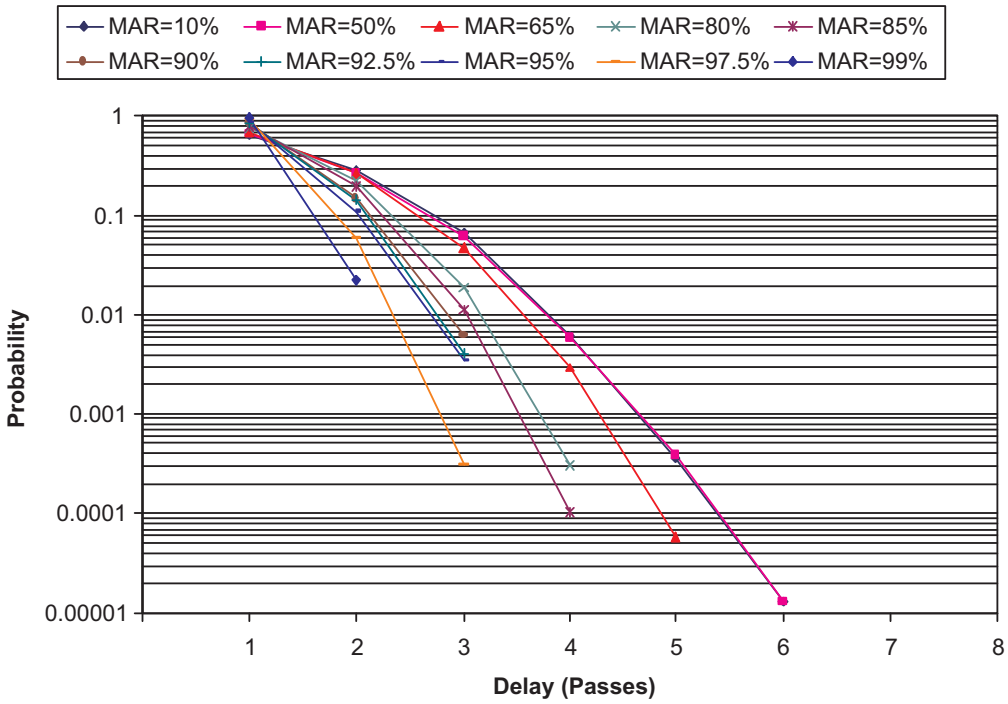

Figure 10. Ka-band Delay Distributions for p_d=0.97 and Different MAR Values

should only be slightly greater than the maximum amount of data that is collected between two passes.

IV. Conclusions and Caveats

IV.A. Conclusions

In this paper, the delay-throughput characteristics of the deep-space Ka-band and deep-space X-band links were obtained through an emulation process using parameters for MRO X-band and Ka-band telecommunication capabilities, MRO tracking schedule and trajectory, parameters for DSN Ka-band antennas and atmospheric noise temperature measurement data from WVR/AWVR. The results indicate that except for very low average delay requirements, the deep-space Ka-band link could deliver more than twice the throughput of the X-band link for the same amount of power consumed on the spacecraft with a storage amount less than three times the maximum amount of data that the spacecraft collects between passes.

IV.B. Caveats

This study is subject to several caveats. First of all, the WVR/AWVR data that were used for this study are provided at a rate of roughly one sample per every five minutes. This rate is not sufficient to resolve short time scale variations on the link. Therefore, if such short time scale variations actually exist, the result could look significantly different.

Next, the results are provided for roughly one pass per complex per week. Such a time sampling does not capture the effects that a weather system could have over several consecutive days at a complex, since most weather systems do not affect an area for more than two or three days. Given this, the average delay and the

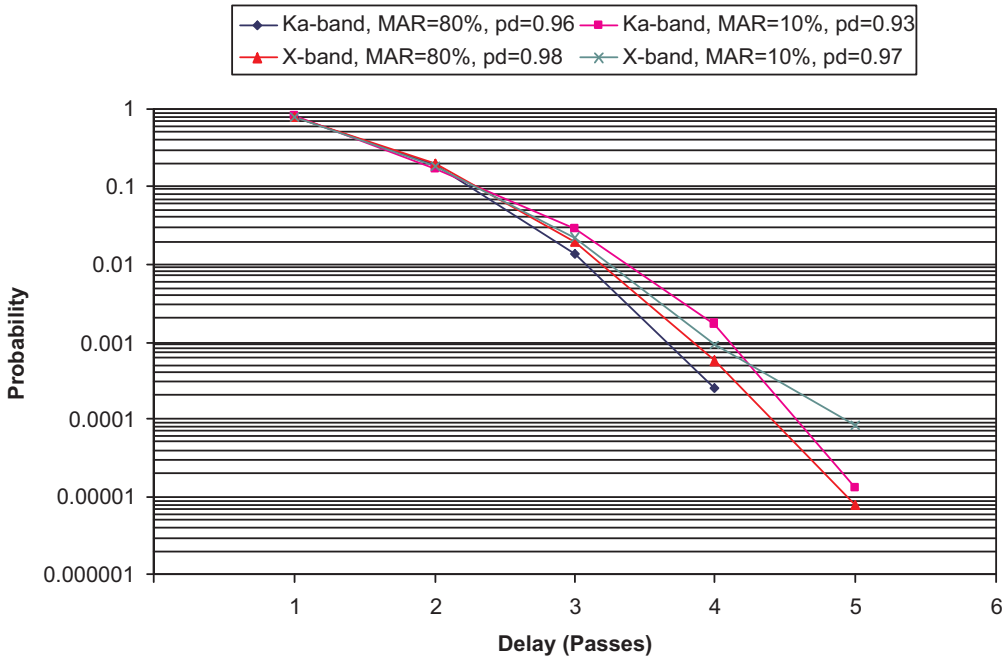

Figure 11. Delay Distributions for Different X-band and Ka-band Link Configurations with Similar Average Delays

spacecraft storage could increase if the passes are scheduled much closer together. In addition, this analysis does not take into account ground antenna degradations that are caused by the environment. While, based on our experience with MRO during its cruise phase,[1] the active ground antenna pointing seems to work very well even under very windy conditions, other factors such as wind loading of the antenna which causes a degradation in the antenna gain have been ignored mostly because of incomplete modeling of them. If these effects are substantial, the advantage that the Ka-band shows over X-band could be reduced. Finally, the advantage shown for Ka-band over X-band is dependent on the efficiency of the spacecraft power amplifiers that are used. Typically, for the same RF transmitted power, the higher frequency amplifiers are less efficient than the lower frequency amplifiers. Furthermore, as the RF output power of the amplifier increases, so does its efficiency. Therefore, the Ka-band system could have more of an advantage over the X-band than shown for higher output RF power levels and less of an advantage for lower output RF power levels.

Acknowledgments

This work was performed at Jet Propulsion Laboratory (JPL), California Institute of Technology, under a contract with National Aeronautics and Space Adminstration. The author would like to thank the Interplanetary Network Directorate (IND) at JPL for programmaitic support of this task. The author would also like to thank Steve Keihm of JPL for processing the WVR and AWVR data. Finally, thanks go to David Morabito, Jon Hamkins, Fabrizio Pollara, Wallace Tai and Yuhsyen Shen of JPL for their advice and support.

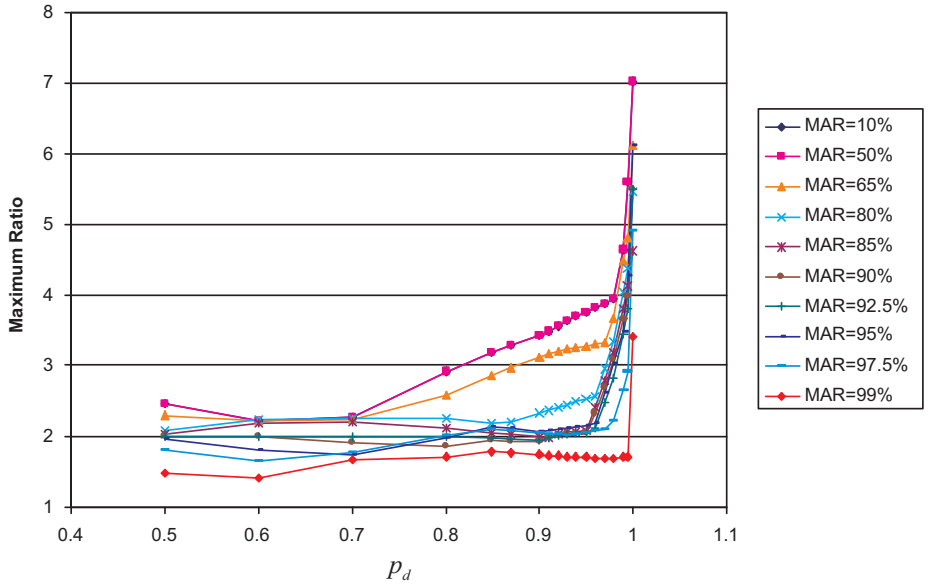

Figure 12. Maximum Ratio of Buffer Size at the Beginning of the Pass to the Amount of Data Collected Before the Pass vs. p_d for Different MAR Values, Ka-band

References

[1]S. Shambayati, J. S. Border, D. D. Morabito and R. Mendoza, "MRO Ka-band Demonstration: Cruise Phase Lessons Learned," *IEEE Aerospace Conference*, Big Sky, Montana, March 3-10, 2007.

[2]R. W. Sniffin, Ed., *DSMS Telecommunications Link Design Handbook (810-005, Rev. E)*, Module 104, Rev. B: 34-m BWG Stations Telecommunications Interfaces, *http://deepspace.jpl.nasa.gov/dsndocs/810-005/104/104B.pdf*, Jet Propulsion Laboratory, Pasadena, CA, August 1, 2005.

[3]S. Shambayati, "Deep-Space Ka-band Link: Design, Continuity and Completeness," *IEEE Aerospace Conference*, Big Sky, Montana, March 2-7, 2008.

[4]S. Shambayati, D. Morabito, J. S. Border, F. Davarian, D. K. Lee, R. Mendoza, M. Britcliffe and S. Weinreb, "Mars Reconnaissance Orbiter Ka-band (32 GHz) Demonstration: Cruise Phase Operations," *Spaceops 2006 Conference*, Rome, Italy, June 2006, pp. 1-26

[5]Consultative Committee for Space Data Systems Informational Report 130.1-G-1, *TM Synchronization and Channel Coding- Summary of Concept and Rationale*, Issue 1,*http://public.ccsds.org/publications/archive/130x1g1e1.pdf*, Washington, D.C., June 2006

[6]S. Shambayati, "Ka-Band Telemetry Operations Concept: A Statistical Approach," *Proceedings of the IEEE*, Volume 95, Issue 11, Nov. 2007, pp. 2171 - 2179

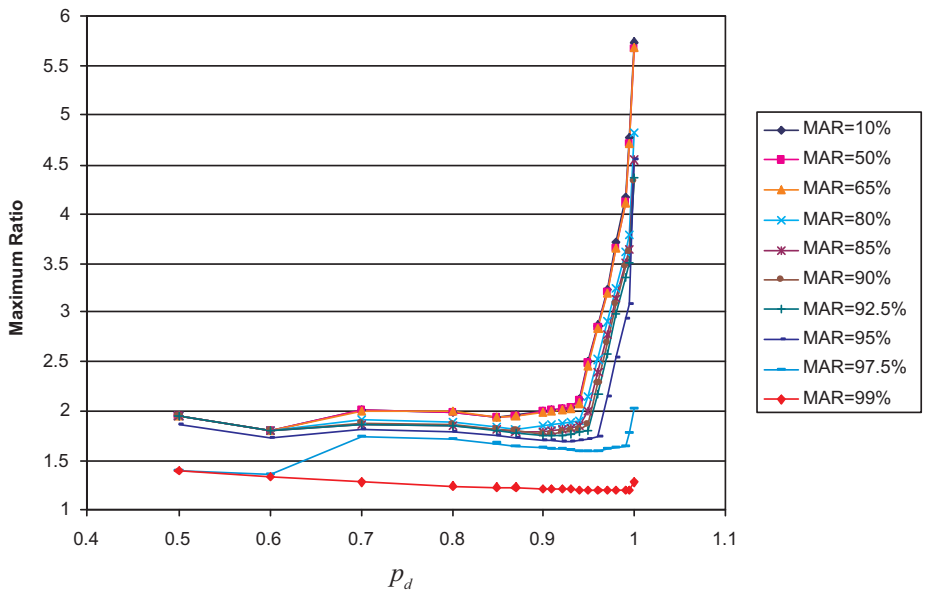

Figure 13. Maximum Ratio of Buffer Size at the Beginning of the Pass to the Amount of Data Collected Before the Pass vs. p_d for Different MAR Values, X-band

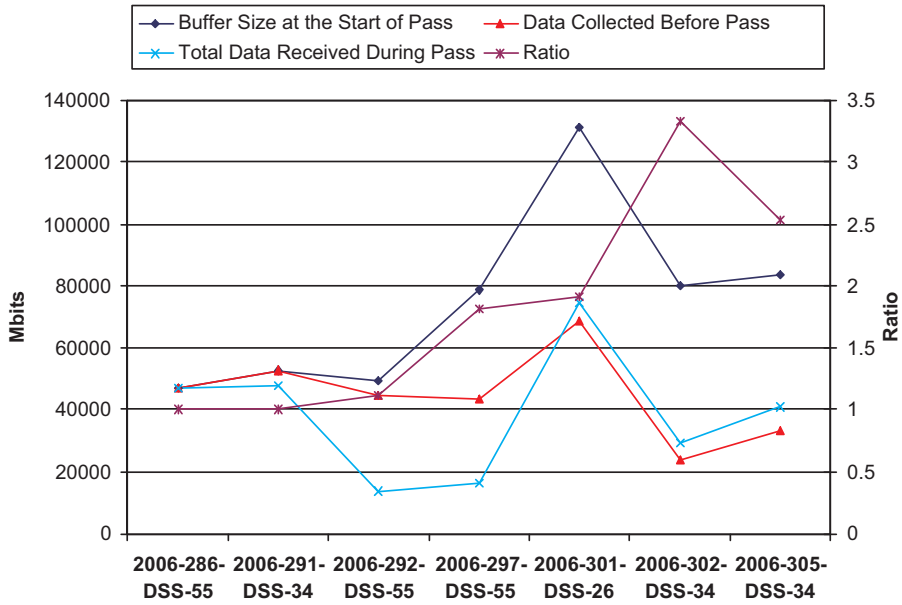

Figure 14. Buffer Size at the Beginning of the Pass, Data Collected Before the Pass, Data Received Correctly During the Pass and the Ratio of the Buffer Size at the Beginning of the Pass to the Data Collected Before the Pass, Ka-band Link, MAR= 65%, p_d=0.97.

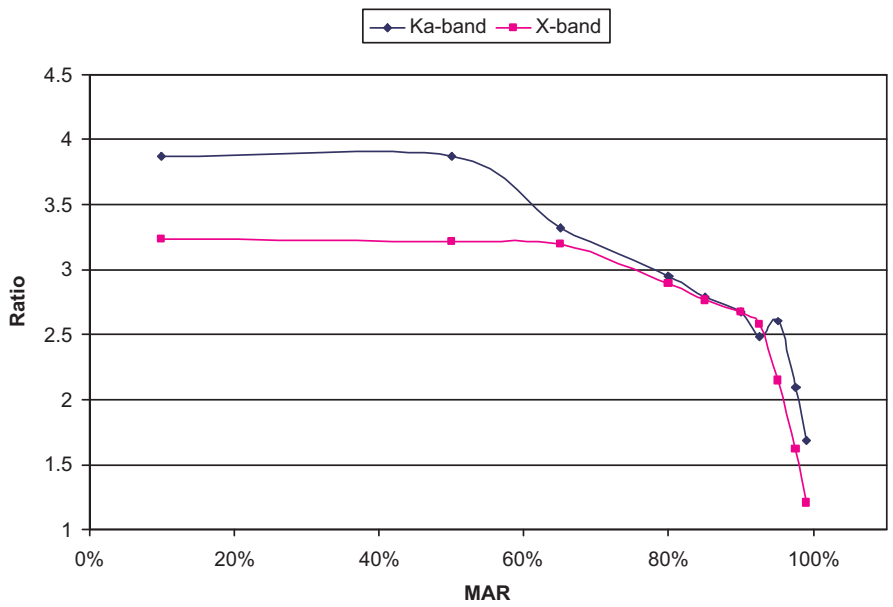

Figure 15. Maximum of Ratio of the Buffer Size at the Beginning of the Pass to the Data Collected Before the Pass for Different MAR Values, Ka-band and X-band, p_d=0.97.